

Automatic land cover classification with SAR imagery and Machine learning using Google Earth Engine

Original Scientific Paper

Geeta T. Desai

Department of Electronics and Telecommunication,
Babasaheb Naik College of Engineering, Pusad, Maharashtra, India.
tgeetadesai@gmail.com

Abhay N. Gaikwad

Department of Electronics and Telecommunication,
Babasaheb Naik College of Engineering, Pusad, Maharashtra, India.
abhay.n.gaikwad@gmail.com

Abstract – Land cover is the most critical information required for land management and planning because human interference on land can be easily detected through it. However, mapping land cover utilizing optical remote sensing is not easy due to the acute shortage of cloud-free images. Google Earth Engine (GEE) is an efficient and effective tool for huge land cover analysis by providing access to large volumes of imagery available within a few days after acquisition in one consolidated system. This article demonstrates the use of Sentinel-1 datasets to create a land cover map of Pusad, Maharashtra using the GEE platform. Sentinel-1 provides Synthetic Aperture Radar (SAR) datasets that have a temporally dense and high spatial resolution, which is renowned for its cloud penetration characteristics and round-the-year observations irrespective of the weather. VV and VH polarization sentinel-1 time series data were automatically classified using a support vector machine (SVM) and Random Forest (RF) machine learning algorithms. Overall accuracies (OA), ranging from 82.3% to 90%, were obtained depending on polarization and methodology used. RF algorithm with VV polarization dataset stands better in comparison to SVM achieving OA of 90% and Kappa coefficient of 0.86. The highest user accuracy was obtained for the water class with both classifiers.

Keywords: Land cover classification, Google Earth Engine, Synthetic aperture radar, Random Forest and Support vector machine

1. INTRODUCTION

Land cover (LC) is the physical surface of earth consisting of water, agriculture, soil, forest and other physical features of the earth's surface [1]. Availability of precise and timely global and regional level LC mapping information is vital for environmental monitoring, precision agriculture, urban planning and others [2-4]. LC classification and vegetation mapping information is crucial for policy making to help farmers for planning their agricultural resources. This makes the LC and vegetation mapping a key factor in environmental studies [5]. Due to the large scale and free availability of remotely sensed data, it has gained recognition as a prominent data source for LC mapping over the time [6]. In literature a number of LC classification studies are carried out using sentinel2 optical and sentinel1 radar sensors. LC mapping utilizing optical remote sensing is a difficult task due to acute shortage of cloud-free images [7]. Uninterrupted, round-the-clock observations of Sentinel-1A in all weather con-

ditions make it a preferred data source for land monitoring, especially in areas having continuous cloud cover [8]. Sentinel-1A (S1A), operates with a revisit interval of 12-day, 20m spatial resolution, and with two polarizations vertical transmit, vertical receive (VV) and vertical transmit, horizontal receive (VH) [8].

Google Earth Engine (GEE) is recognized as a cloud-based computing platform having immense capacity for processing, storage and integration of satellite data. The availability of different state of art classifiers and fast processing speed have made GEE more popular among researchers [9].

Machine learning (ML) is an effective and efficient methodology for remote sensing applications. Over the last two decades there have been substantial advancements in developing ML based approaches for LC mapping using remote sensing imagery [10, 11]. Support vector machine (SVM) classifiers have received more attention in earth science applications due to their

efficient performance with limited training data [12]. Popularity of Random Forest (RF) has increased in the remote sensing field due to its excellent classification accuracy and processing speed [13]. The aim of the paper is to quantify the ability of Sentinel-1A dataset for the LC type mapping utilizing ML algorithms like SVM and RF on the Google Earth Engine (GEE) platform and compare their performance using user accuracy (UA), producer accuracy (PA) overall accuracy (OA) and F1 score. The rest of the article is structured as follows: In section 2 short review on LC mapping using SAR is covered.

In section 3 study area is introduced. In section 4 methodology used is presented while in section 5 experimental results, conclusion and future work are discussed.

2. RELATED WORK

Over the past decade, there is growing interest in the LC classification using remote sensing techniques due to its importance in different applications related to environmental studies. The SAR imagery has been used by many researchers for getting information about the type of land cover.

In [14] authors have presented the use of Sentinel-1 data to classify four classes of LC in the province of Punjab located in Pakistan, the results of the study concluded that joint use of coherence with backscattered intensity improves the accuracy of the classification to obtain 80% overall accuracy.

In [15] authors have highlighted that joint use of features from ascending and descending orbit dual-polarized images of Sentinel-1 increases classification accuracy than using a single pass image.

In [16] authors have analysed the use of multisource and multitemporal SAR imagery to improve classification accuracy in wetlands using a multiple classifier system.

In [17] authors have used a combination of ascendant and descendant orbit images keeping both polarizations of SAR data for the finding of the built-up areas.

In [18] authors have evaluated the potential of Sentinel-1A data by combining different attributes extracted from backscatter, polarimetry, and interferometry using RF and SVM classifiers for LC mapping of the Amazon region. Authors discriminated artificial surfaces, forests, and non-forested areas using multitemporal SAR data taken over small observation intervals of time. UA of 91% was obtained.

In [19] authors have highlighted the use of statistical properties of SAR images by using a statistical convolution neural network for LC classification.

In [20] authors have proposed the SAR LC classification approach which is based on region based classification to boost classification accuracy.

In [21] authors have confirmed the capabilities of interferometric SAR signatures for LC mapping in the mountainous area using k-principal component analysis and SVM.

In [22] authors have reported the use of Sentinel-1 interferometric coherence for LC mapping utilizing multiple feature based classifiers and concluded that the coherence information is important for LC mapping and gives better accuracies for all evaluated cases.

In [23] Patric H. et.al introduced Eurosat novel dataset for LC classification consisting of Sentinel-2 images. The dataset covers 13 spectral bands made up of total 27,000 labelled and geo-referenced images for 10 classes.

Generating large-scale land cover maps requires multitemporal satellite data which gives rise to a tremendous amount of data [24]. Processing of big data needs massive storage capacity and access to powerful computational capability. This process becomes a tedious and time consuming task if traditional methods for image collection, filtering, downloading, and preprocessing are used [25]. To support this requirement huge amount of storage, access to high power computing and flexibility to implement diverse applications are required. All the above requirements were taken care of after the emergence of the open access GEE platform.

GEE, is an integrated cloud-based computing platform that comes with a powerful capability of Google and can resolve the prominent issues related to the LC mapping of huge study regions [9]. Users can process large volumes of remote sensing data without the need to download it to their machine on GEE web-based Integrated Development Environment code editor [25]. The Availability of different algorithm packages and fast processing makes GEE more popular among researchers [26].

GEE has become an asset to the remote sensing community by making satellite data processing very convenient and fast.

Researchers are utilizing GEE in recent years for LC classification. The use of GEE for land cover classification using Landsat8 [24,25,27,28], Sentinel2 [29] and combinations of Sentinel2 and Landsat8[30] has shown good results. Therefore GEE presents great opportunities in dealing with remote sensing data for LC mapping in Pusad. Till date, most studies using GEE for LC mapping are focused on using Landsat and Sentinel2 optical images. There are few studies that used SAR imagery for large-scale LC mapping using ML methods on the GEE platform.

3. STUDY AREA

Pusad is a small city in the central area of Maharashtra state in India, which lies on latitude 19.912676, and longitude 77.566910 and includes the Pus River.

Pusad has a total area of approximately 1176 sq. kms. The prime LC in the study area is agriculture and the prominent crops grown are wheat, soybean, cotton, and turmeric, extending over a total 65% of the area under investigation. In addition to agriculture, the study area also contains urban areas, trees and water bodies. All agricultural areas are grouped into a single class called agriculture. Other remaining classes are urban area, vegetation, water and bare soil. Fig. 2 shows a backscatter image of the Pusad region in VV and VH polarization.

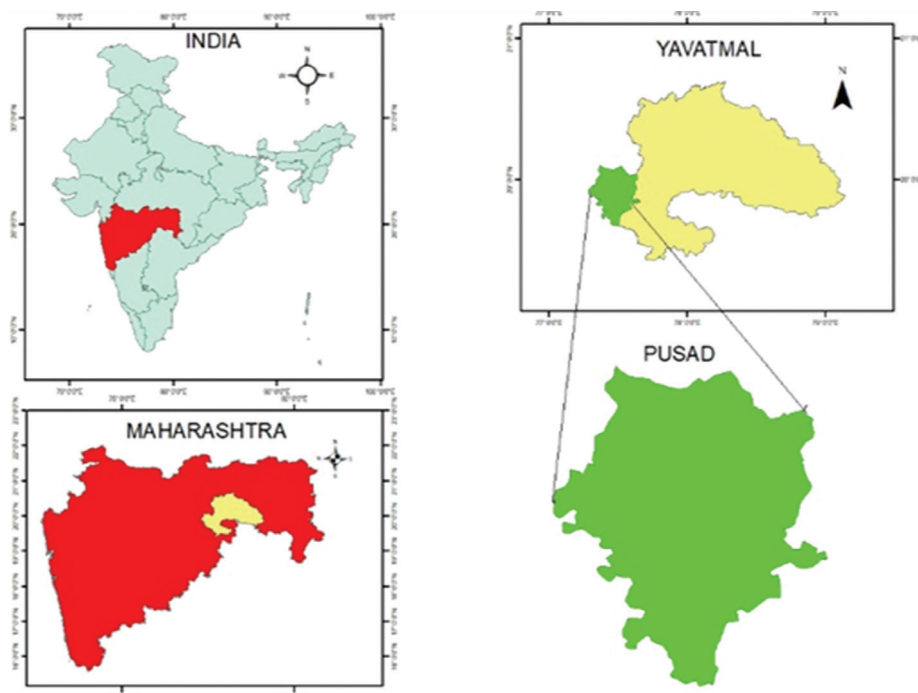


Fig. 1. Location Map of Pusad, India

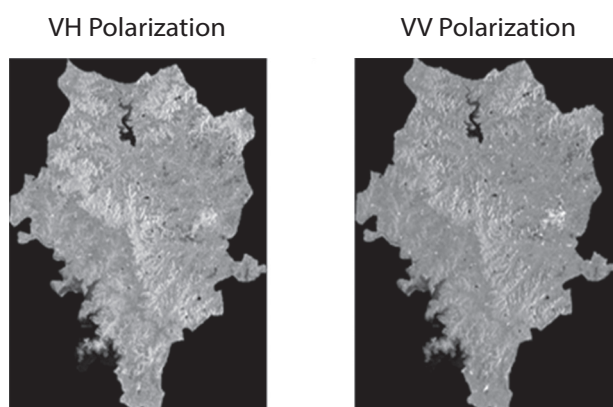


Fig. 2. Backscatter image of study area for VV and VH band

4.1 SENTINEL1 SAR IMAGE AND PREPROCESSING

In this study, the sentinel1- SAR GRD dataset of the study area stored in the GEE cloud platform was used and it included all images covering the area of investigation in the time period from January to April of the years 2018, 2019 and 2020. The Sentinel-1 SAR GRD

4. METHODOLOGY

Fig.3 flowchart describes the methodology used for exploring the LC classification in the study area. The methodology is organized into three stages. In the first stage, SAR images of the study area are acquired and pre-processed. The second stage deals with defining classification classes and the selection of training samples. In the last stage, classification and evaluation of the algorithm are performed.

dataset was acquired using the interference wide-band (IW) mapping mode, with a spatial resolution of 20 m, a width of 250 km, and an average incidence angle of 30–45 with a 12 day revisit time. The dataset contains VV and VH polarization. Sentinel-1 image preprocessing was implemented using GEE. Preprocessing includes orbit restitution, thermal noise removal, terrain correction and radiometric calibration. Each sentinel1 image was filtered to reduce speckle on the GEE platform [31].

4.2 TRAINING CLASSIFIER

Five types of LC i.e. agriculture, barren land, urban, vegetation, and water are the dominant part of the study area. Training and validation data was selected depending on human visual interpretation of high-resolution images from GEE [25,32]. Two popular supervised classifiers SVM and RF were deployed for LC mapping in Pusad.

4.2.1 SVM

SVM is a type of supervised learning, non-parametric classifier algorithm mostly used due to its ability to

work with limited training datasets with good classification results [33,34]. SVM training classifiers find an ideal hyperplane in the training phase that divides the dataset into predefined numerous classes with a few misclassified pixels. SVM uses support vectors to create the hyperplane. Support vectors are selected based on the cost parameter, Gamma, and kernel functions. The grid search based optimization technique is used to select C and Gamma parameters, producing trustworthy prediction outcomes. The random basis kernel is preferred for training on large datasets [33].

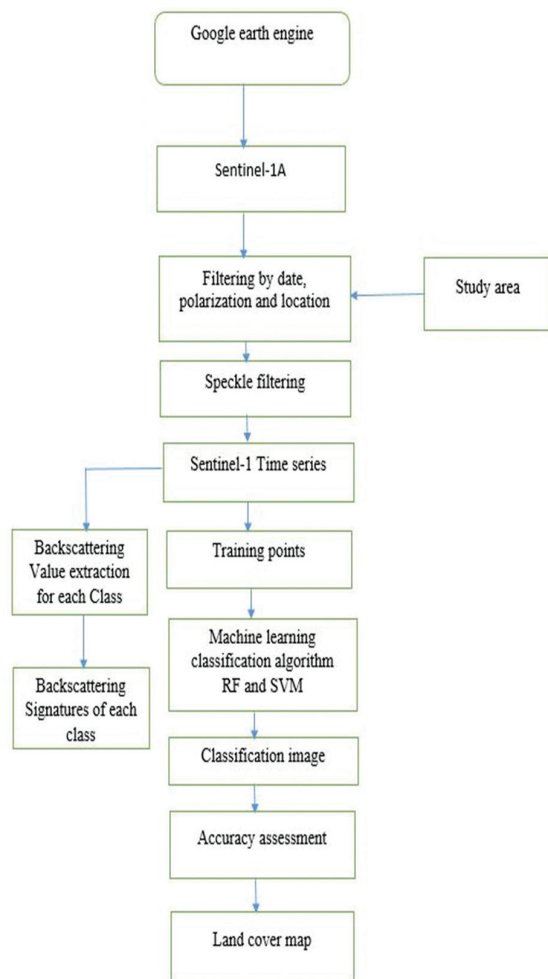


Fig. 3. Flowchart of methodology

4.2.2. Random Forest

RF is a type of ensemble classification technique. RF is found appealing to researchers in remote sensing over the last decade due to the identification and better handling of outliers in training samples using sample proximity measurement techniques [35,36]. RF performs well with highly correlated hyperspectral data as compared to other streamlined ML classifiers. Another factor that makes RF a favorite of researchers is that it requires the setting of only two parameters n_{tree} and m_{try} [10,37]. Taking into account all the above reasons we chose RF as one of the classification algorithms. As per suggestions of previous studies, we have set n_{tree} parameter to 100 and m_{try} was set to the default value.

After completion of classification, an assessment step was performed for evaluating classification algorithms. Out of the total dataset, 70 percent was used for training the algorithm and the remaining 30 percent was used as a testing dataset. The OA, Kappa coefficient, UA and PA of each class was calculated using the inbuilt algorithm from GEE.

5. RESULTS AND DISCUSSIONS

5.1 TEMPORAL BACKSCATTER PATTERNS OF DIFFERENT LAND COVERS

Fig. 4 summarizes temporal backscatter signature curves of VV and VH bands for each land cover type in 2020. In the graph, the date on which the image is acquired is plotted on X-axis and backscattering coefficient is plotted on Y-axis. The average backscatter value was extracted from each image belonging to each LC class. From Fig. 4 it is observed that

i) Lowest backscatter values in VV and VH bands were noticed in the case of water bodies. Moreover, the urban class showed the maximum backscatter values for VV and VH bands.

(ii) Vegetation showed constant backscatter values throughout the time of image acquisition with slight variation in the month of September and October. The backscatter of the agricultural class showed more variation with VH.

(iii) Backscattering curves of vegetation and barren land showed similar shapes therefore identification of these classes was difficult.

5.2 LAND COVER CLASSIFICATION OF PUSAD

This study examines the potential of SVM and RF classifiers for LC classification using SAR images on the GEE platform. Fig. 5 and 6 present the classification results of VV and VH polarization using SVM and RF techniques for the year 2018. The accuracy assessment parameters showed variation in results with polarization and classifier.

In several studies [15 -23] authors processed remote sensing data on third party software, we implemented the entire methodology inside the GEE platform and used the JavaScript language for programming in the code editor. Analysing high volume data with remote sensing software on a personal computer is a tedious task however it is easily manageable on GEE. Hence GEE offers an attractive solution to users having low end devices to obtain satisfactory results in less time without the need of high power computers or commercial software. Most researchers previously used Landsat [24,25,27,28], Sentinel-2 [29] and a combination of Landsat and sentinel-2[30] images for generating LC classification. We chose sentinel-1 images since SAR sensors can acquire an image in all weather conditions in addition to these different combinations of wavelength and polarization provides important information regarding the earth's surface [26].

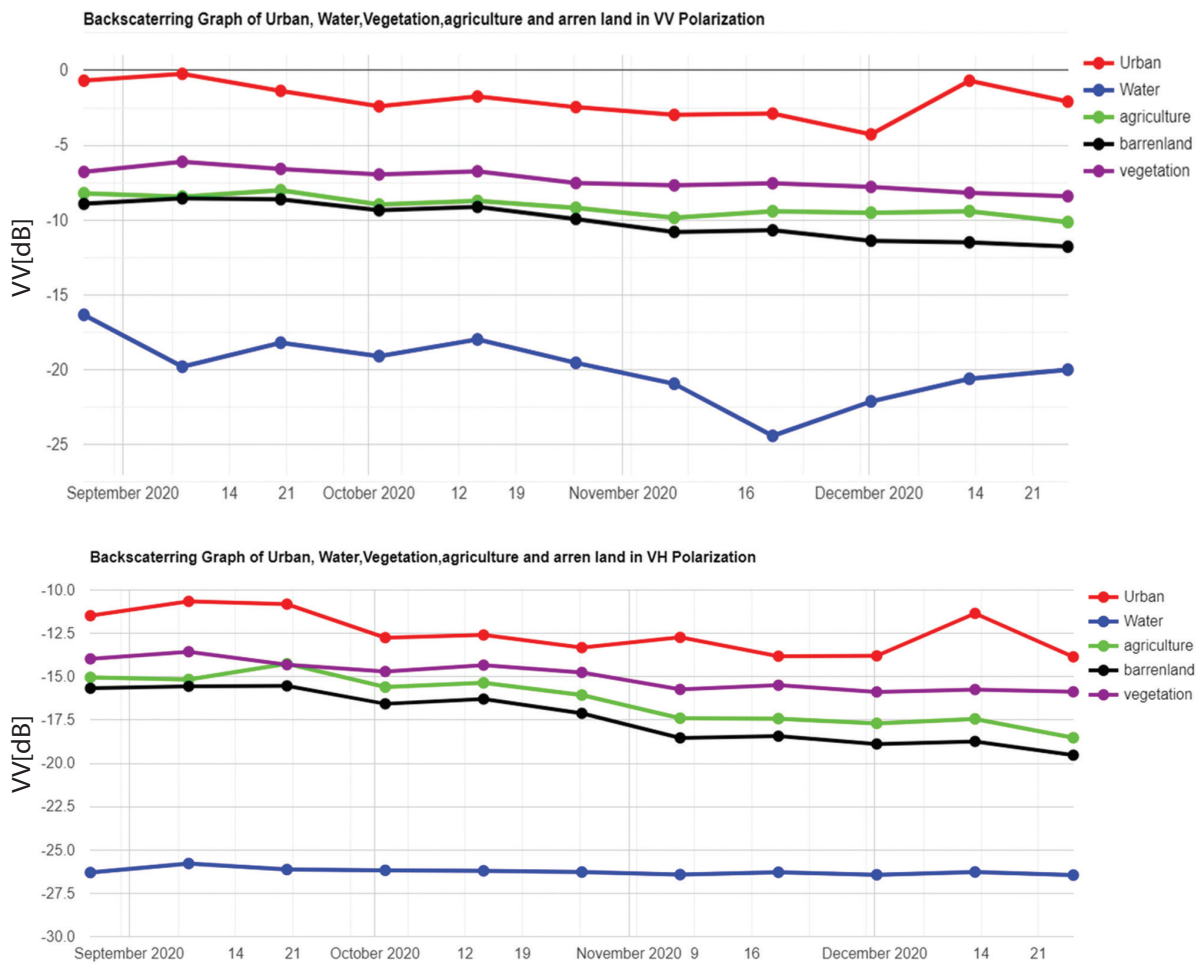


Fig. 4. Temporal backscatter profiles for five different land cover classes for VV and VH

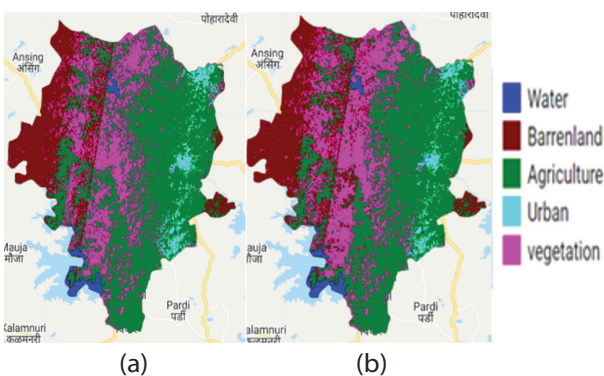


Fig. 5 . LC output Using RF for year 2018 for VH(a) and VV(b) band

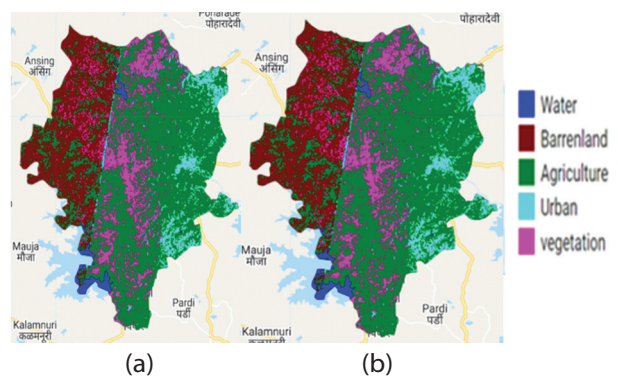


Fig. 6. LC output using SVM for year 2018 for VH(a) and VV(b) band

Table 1, Table 2, Table 3 and Table 4 show the results of the SVM and RF classifier. UA, and PA, F1 score were used to assess the class wise performance of each classifier. Both the classifiers get confused between barren land and vegetation areas however their performance for water, agriculture, and urban class is better. From the classification result it can be observed that most of the barren land is getting misclassified as an urban area.

Our results show that RF has proved superior to the SVM classifier in line with results obtained in [26] Tak-

ing into account accuracies summarized in Table 2, it is clear that barren land and vegetation area are mostly misclassified classes. For SVM and RF, the performance of the water class was best as compared to other classes in agreement with the results obtained in [30]. Obtained results claim that VV polarization performs better in comparison to the VH band and similar results were found in [16]. From results it is observed that RF outperforms SVM in LC applications due to its robustness to outliers and noise also as compared to RF SVM is more sensitive

to hyperparameters [38]. Obtained results show that the presented approach achieves improvement of 3% in overall accuracy for land cover classification compared to obtained in [28] since SAR sensors can acquire an image in all weather conditions in addition to these different combinations of polarization provides important LC details of the earth's surface which improves LC classification accuracy.

As shown in the Fig. 7, SVM achieved an accuracy of OA between 86.49% and 82% and kappa between 0.75 and 0.81 for the images from 2018 to 2020. While the RF achieved accuracy of OA between 90% and 85.8%, and kappa between 0.80 and 0.86 for the images from 2018 to 2020. The average kappa coefficient for SVM and RF was 0.78 and 0.83 respectively. The dominant LC in the study area is agriculture, barren land and vegetation. Considering the results of RF algorithm for VV polarization it can be concluded that from 2018 to 2020, urban coverage and barren land showed a commutative increase by 1.1% and 2.3% of the study area respectively. From 2018 to 2020 vegetation area including forests and grasslands showed a reduction of 4.9% of the study area. Agricultural was seen most dominant class in 2019 as compared to 2020.

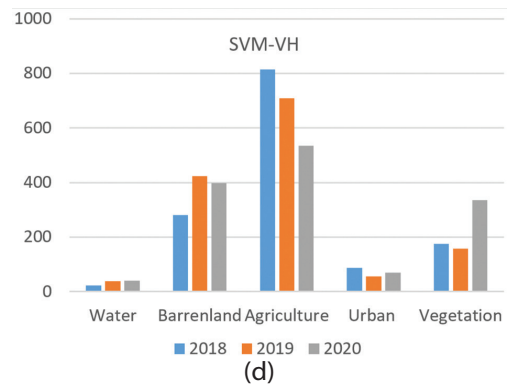
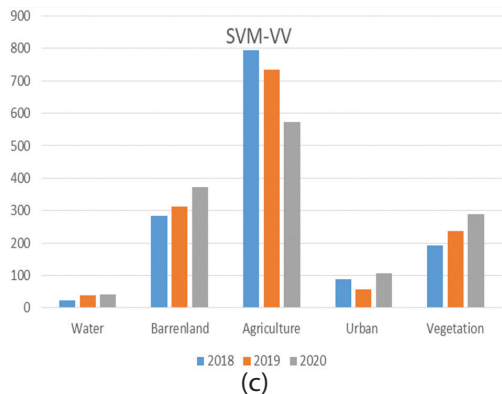
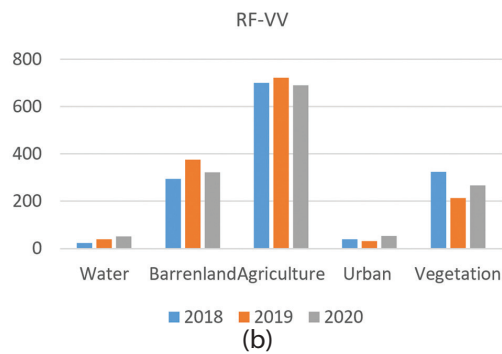
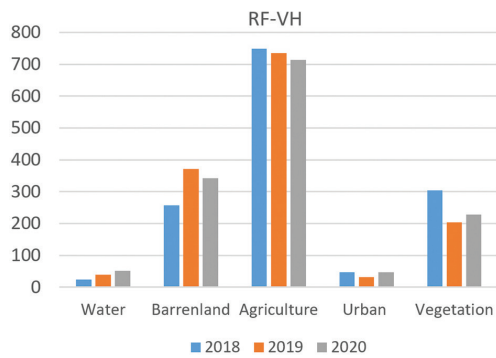


Fig. 7. Areas of water, Barrenland, Agriculture, urban and vegetation for 2018, 2019 and 2020.

Table 1. Comparison between SVM and RF classifier using Kappa coefficient and overall accuracy.

Year	Classifier	VV Band		VH Band	
		OA	Kappa Coefficient	OA	Kappa Coefficient
2018	SVM	86.49	0.818	85.3	0.79
	RF	90	0.86	89	0.85
2019	SVM	85.43	0.80	82.3	0.75
	RF	89	0.84	88	0.84
2020	SVM	85.71	0.805	83.27	0.77
	RF	85.8	0.80	87.5	0.83

Table 2. User accuracy and producer accuracy of each class for 2018 using RF and SVM

Class	RF		SVM	
	PA	UA	PA	UA
Water	93	97	98.60	94
Barren land	81	75	62.35	54
Agriculture	94.59	92	89.64	94.68
Urban	94.55	97	91.56	93.82
Vegetation	81.25	81	79.50	75.78

Table 3. User accuracy and producer accuracy of each class for 2018 using RF and SVM

Class	VV Band			VH Band		
	Precision	Recall	F1	Precision	Recall	F1
Water	97	93	95	94	99	96
Barren land	75	81	78	71	80	75
Agriculture	92	94.59	93	94	93	93
Urban	97	94.44	96	100	94	96
Vegetation	81	81.25	81	83	77	79

Table 4. Precision, Recall and F1 score of each class for 2018 using SVM classifier

Class	VV Band			VH Band		
	Precision	Recall	F1	Precision	Recall	F1
Water	97	93	95	94	99	96
Barren land	75	81	78	71	80	75
Agriculture	92	94.59	93	94	93	93
Urban	97	94.44	96	100	94	96
Vegetation	81	81.25	81	83	77	79

6. CONCLUSION:

The study evaluated the performance of RF and SVM for LC classification using time series Sentinel-1A datasets on the GEE platform for Pusad region. LC classification using SVM with VV gave overall accuracy of 85.87% with a kappa coefficient of 0.80, while classification with VH band gave an accuracy of 83.62% with a kappa coefficient of 0.77. With RF classifier VV gave overall accuracy of 88.26% with a kappa coefficient of 0.84 while with VH band overall accuracy of 88.1% with Kappa coefficient of 0.84 is obtained. Based on the results it can be concluded that RF classifier using VV band gave best results. Agricultural and barren land is the main land cover types in the Pusad region. Future work can be focused on deep learning methodologies for LC mapping.

7. REFERENCES:

- [1] J. S. Rawat, M. Kumar, "Monitoring land use/cover change using remote sensing and GIS techniques: A case study of Hawalbagh block, district Almora, Uttarakhand, India", *The Egyptian Journal of Remote Sensing and Space Science*, Vol. 18, No. 1, 2015, pp. 77-84.
- [2] C. Zhang, J. M. Kovacs, "The application of small unmanned aerial systems for precision agriculture: a review", *Precision agriculture*, Vol. 13, No. 6, 2012, pp. 693-712.
- [3] H. Shi et al. "Accurate urban area detection in remote sensing images", *IEEE Geoscience and Remote Sensing Letters*, Vol. 12, No. 9, 2015, pp. 1948-1952.
- [4] Y. A. Liou, A. K. Nguyen, M. H. Li, "Assessing spatio-temporal eco-environmental vulnerability by Landsat data", *Ecological Indicators*, Vol. 80, 2017, pp. 52-65.
- [5] R. S. DeFries, J. R. G. Townshend, "NDVI-derived land cover classifications at a global scale", *International journal of remote sensing*, Vol. 15, No. 17, 1994, pp. 3567-3586.
- [6] N. Sidhu, E. Pebesma, G. Câmara, "Using Google Earth Engine to detect land cover change: Singapore as a use case", *European Journal of Remote Sensing*, Vol. 51, No. 1, 2018, pp. 486-500.
- [7] C. Liu, Z.-X. Chen, S. H. A. O. Yun, J. Chen, T. Hasi, H. Pan, "Research advances of SAR remote sensing for agriculture applications: A review", *Journal of integrative agriculture*, Vol. 18, No. 3, 2019, pp. 506-525.
- [8] P. Potin et al. "M.Sentinel-1 mission status", *Proceedings of the EUSAR 2016: 11th European Conference on Synthetic Aperture Radar*, Hamburg, Germany, 6-9 June 2016, pp. 1-6.
- [9] N. Gorelick et al. "Google Earth Engine: Planetary-scale geospatial analysis for everyone", *Remote Sensing of Environment*, Vol. 202, 2017, pp. 18-27.
- [10] A. E. Maxwell, T. A. Warner, F. Fang, "Implementation of machine-learning classification in remote sensing: An applied review", *International Journal of Remote Sensing*, Vol. 39, No. 9, 2018, pp. 2784-2817.
- [11] D. J. Lary, A. H. Alavi, A. H. Gandomi, A. L. Walker, "Machine learning in geosciences and remote sensing", *Geoscience Frontiers*, Vol. 7, No. 1, 2016, pp. 3-10.
- [12] P. Mantero, G. Moser, S. B. Serpico, "Partially supervised classification of remote sensing images through SVM-based probability density estimation", *IEEE Transactions on Geoscience and Remote Sensing*, Vol. 43, No. 3, 2005, pp. 559-570.
- [13] V. F. Rodriguez-Galiano, B. Ghimire, J. Rogan, M. Chica-Olmo, J. P. Rigol-Sanchez, "An assessment of the effectiveness of a random forest classifier for land-cover classification", *ISPRS journal of photogrammetry and remote sensing*, Vol. 67, 2012, pp. 93-104.
- [14] R. Z. Khalil, "InSAR coherence-based land cover classification of Okara, Pakistan", *The Egyptian Journal of Remote Sensing and Space Science*, Vol. 21, 2018, pp. S23-S28.
- [15] S. A. Sayedain, Y. Maghsoudi, S. Eini-Zinab, "Assessing the use of cross-orbit Sentinel-1 images in land cover classification", *International Journal of Remote Sensing*, Vol. 41, No. 20, 2020, pp. 7801-7819.
- [16] M. Amani, B. Salehi, S. Mahdavi, B. Brisco, M. Shehata, "A Multiple Classifier System to improve mapping complex land covers: A case study of wetland classification using SAR data in Newfoundland, Canada", *International Journal of Remote Sensing*, Vol. 39, No. 21, 2018, pp. 7370-7383.
- [17] I.-H. Holobacă, K. Ivan, M. Alexe, "Extracting built-up areas from Sentinel-1 imagery using land-cover classification and texture analysis", *International Journal of Remote Sensing*, Vol. 40, No. 20, 2019, pp. 8054-8069.
- [18] J. M. F. Diniz, F. F. Gama, M. Adami, "Evaluation of polarimetry and interferometry of sentinel-1A SAR data for land use and land cover of the Brazilian Amazon Region", *Geocarto International*, Vol. 37, No. 5, 2022, pp. 1482-1500.

- [19] X. Liu, C. He, Q. Zhang, M. Liao, "Statistical convolutional neural network for land-cover classification from SAR images", *IEEE Geoscience and Remote Sensing Letters*, Vol. 17, No. 9, 2019, pp. 1548-1552.
- [20] M. D. Soares et al. "A meta-methodology for improving land cover and land use classification with SAR imagery", *Remote Sensing*, Vol. 12, No. 6, 2020, pp. 961.
- [21] H.W. Yun, J.-R. Kim, Y.-S. Choi, S.-Y. Lin, "Analyses of time series InSAR signatures for land cover classification: case studies over dense forestry areas with L-band SAR images", *Sensors*, Vol. 19, No. 12, 2019, pp. 2830.
- [22] A. Jacob et al. "Sentinel-1 InSAR coherence for land cover mapping: A comparison of multiple feature-based classifiers", *IEEE Journal of Selected Topics in Applied Earth Observations and Remote Sensing*, Vol. 13, 2020, pp. 535-552.
- [23] P. Helber, B. Bischke, A. Dengel, D. Borth, "EuroSAT: A novel dataset and deep learning benchmark for land use and land cover classification", *IEEE Journal of Selected Topics in Applied Earth Observations and Remote Sensing*, Vol. 12, No. 7, 2019, pp. 2217-2226.
- [24] H. Shafizadeh-Moghadam, M. Khazaei, S. K. Alavipanah, Q. Weng, "Google Earth Engine for large-scale land use and land cover mapping: an object-based classification approach using spectral, textural and topographical factors", *GIScience & Remote Sensing*, Vol. 58, No. 6, 2021, pp. 914-928.
- [25] T. N. Phan, V. Kuch, L. W. Lehnert, "Land Cover Classification using Google Earth Engine and Random Forest Classifier—The Role of Image Composition", *Remote Sensing*, Vol. 12, No. 15, 2020, pp. 2411.
- [26] H. Tamiminia, B. Salehi, M. Mahdianpari, L. Quackenbush, S. Adeli, B. Brisco, "Google Earth Engine for geobig data applications: A meta-analysis and systematic review", *ISPRS Journal of Photogrammetry and Remote Sensing*, Vol. 164, 2020, pp. 152-170.
- [27] N. Wagle et al. "Multi-temporal land cover change mapping using google earth engine and ensemble learning methods", *Applied Sciences*, Vol. 10, No. 22, 2020, p. 8083.
- [28] Md Masroor et al. "Assessing the Influence of Land Use/Land Cover Alteration on Climate Variability: An Analysis in the Aurangabad District of Maharashtra State, India", *Sustainability*, Vol. 14, No.2, 2022, p. 642.
- [29] S. Praticò, F. Solano, S. Di Fazio, G. Modica, "Machine learning classification of mediterranean forest habitats in google earth engine based on seasonal sentinel-2 time-series and input image composition optimisation", *Remote Sensing*, Vol. 13, No.4, 2021, pp. 586.
- [30] K. N. Loukika, V. R. Keesara, V. Sridhar, "Analysis of land use and land cover using machine learning algorithms on google earth engine for Munneru River Basin, India", *Sustainability*, Vol. 13, No.24, 2021, pp. 13758.
- [31] A. Mullissa et al. "Sentinel-1 sar backscatter analysis ready data preparation in google earth engine", *Remote Sensing*, Vol. 13, No.10, 2021, pp. 1954.
- [32] M. C. Hansen et al. "A method for integrating MODIS and Landsat data for systematic monitoring of forest cover and change in the Congo Basin", *Remote Sensing of Environment*, Vol. 112, No.5, 2008, pp.2495-2513.
- [33] G. Mountrakis, J. Im, C. Ogole, "Support vector machines in remote sensing: A review", *ISPRS Journal of Photogrammetry and Remote Sensing*, Vol. 66, No.3, 2011, pp.247-259.
- [34] B.-E. Jamsran et al. "Applying a support vector model to assess land cover changes in the Uvs Lake Basin ecoregion in Mongolia", *Information Processing in Agriculture* Vol. 6, No.1, 2019, pp.158-169.
- [35] X. Li et al., "A comparison of machine learning algorithms for mapping of complex surface-mined and agricultural landscapes using ZiYuan-3 stereo satellite imagery", *Remote Sensing*, Vol. 8, No.6, 2016, pp.514.
- [36] Y. Jin et al. "Land-cover mapping using Random Forest classification and incorporating NDVI time-series and texture: A case study of central Shandong", *International Journal of Remote Sensing*, Vol. 39, No.23, 2018, pp.8703-8723.
- [37] M. Belgiu, L. Drăguț, "Random forest in remote sensing: A review of applications and future directions", *ISPRS Journal of Photogrammetry and Remote Sensing*, Vol. 114, 2016, pp.24-31